SURFACE MEDIATED FLOWS IN GLASS NANOFLUIDIC DEVICES

Shaurya Prakash[*] and M.B. Karacor
Department of Mechanical Engineering, The Ohio State University, Columbus, Ohio, USA

ABSTRACT

In this paper, use of chemical modification to selectively direct flow in glass devices is discussed. Glass devices with a slit-like nanochannel and a depth of 100 nm were fabricated by conventional methods. Velocity profile analysis was performed by manipulating the existing theoretical models to explicitly show influence of surface charge density and changing the electric double layer thickness. Theoretical models predict velocity profiles for a wide range of surface charge densities as function of surface functionalization, electrolyte concentration, and electrolyte pH. In addition, experimental data shows selective flow directing in devices is possible by engineering the surface charge density through chemical modification. Use of fluorescent dyes by using both a positive marker dye and a negative marker dye demonstrate selective flow control as pathway to 'valve-less' flow control. The positive dye shows a preference for the aminated channels, which is the more negative surface in the tested devices.

INTRODUCTION

Nanofluidics finds an important place in Lab-on-Chip applications due to the dominance of interfacial forces [1]. Applications for Lab-on-Chip systems in electrophoretic separations, DNA and protein analyses, and PCR, etc. require exquisite control over analyte and sample manipulation and technologies such as molecular gates [2] and entropic traps have been developed [3] for this purpose. High surface-area-to-volume ratios (~ 10^9 m^{-1} are possible) in nanochannels provide a unique opportunity to exploit surface-species interactions for sample manipulation [4].

Chemically modified surfaces within nanofluidic channels with critical dimensions on the order of 100 nm for surface mediated flow control were fabricated and tested. Chemical modifications were carried out by using methods of 'click' chemistry [5]. The modified surfaces can be used to selectively drive flows in these devices. Therefore, the ability to systematically modify surface properties to directly influence confined flows can be a powerful technology for sample manipulation in nanofluidics. In this paper, pre-designed surface properties (e.g., surface charge and surface energy) were used to demonstrate control over electrokinetically driven nanoscale flow phenomena.

Theoretical Background

It has previously been shown [6] that for a slit-like channel driven by electrokinetic flow, the velocity profile for a steady, no-slip, 1-D flow in the axial direction is governed by

$$\mu \frac{d^2 V_z}{dy^2} + E_z \rho(y) = 0 \tag{1}$$

where, μ is the viscosity of the fluid, V_z denotes the velocity in the z-direction or axial direction along length of channel, E_z is the applied electric field in the axial flow or in the z-direction, and ρ denotes the charge density governed by the Poisson equation

$$\frac{d^2 \psi}{dy^2} + \frac{\rho}{\varepsilon_r \varepsilon_0} = 0 \tag{2}$$

where, ψ denotes the potential, ε_r is the dielectric constant of the medium, and ε_0 is the permittivity of free space. If we assume the Boltzmann distribution for the ions in the channels and apply the low-zeta potential assumption, then the velocity profile is given by

$$V_z(y) = -\frac{E_Z \varepsilon_0 \varepsilon_r \zeta}{\mu}\left(1 - \frac{\cosh(\kappa y)}{\cosh(\kappa a)}\right) \tag{3}$$

where, ζ denotes the zeta potential of the surface, y is the vertical coordinate, a is the channel half-depth, and κ is the electrokinetic radius or the reciprocal of the Debye length, often approximated as the thickness of the electric double layer. On integrating equation (3) along the y-direction for the entire channel depth and dividing through by the channel height, $2a$ the average velocity, V_{avg} is obtained and can be expressed as

$$V_{avg} = -\frac{E_Z \varepsilon_0 \varepsilon_r \zeta}{\mu a}\left(\frac{\kappa a \sinh(\kappa a) - \cosh(\kappa a) + 1}{\kappa \sinh(\kappa a)}\right) \tag{4}$$

It is now established that surface charge is critical to ionic control in nanofluidics [7] as the slip plane may not always be well defined [4], and it is known from Grahame's equation that the ζ potential and surface charge density, σ_s are related,

$$\frac{\sigma_s \lambda_D e}{2\varepsilon_0 \varepsilon_r k_B T} = \sinh\left(-\frac{e\zeta}{2k_B T}\right) \tag{5}$$

where, e is the elementary charge, T is the absolute temperature, k_B is Boltzmann constant, and λ_D is the Debye length. Therefore, the velocities in equations (3) and (4) can be expressed in terms of the surface charge density to yield equations (6).

$$V_z(y) = \frac{2k_B E_Z \varepsilon_0 \varepsilon_r T}{\mu e}\sinh^{-1}\left(\frac{\sigma_s e}{2\kappa\varepsilon_0\varepsilon_r k_B T}\right)\left[1 - \frac{\cosh(\kappa y)}{\cosh(\kappa a)}\right]$$

$$V_{avg} = \frac{2k_B E_Z \varepsilon_0 \varepsilon_r T}{a\mu e}\sinh^{-1}\left(\frac{\sigma_s e}{2\kappa\varepsilon_0\varepsilon_r k_B T}\right)\left[\frac{\kappa a \sinh(\kappa a) - \cosh(\kappa a) + 1}{\kappa \sinh(\kappa a)}\right] \tag{6}$$

Therefore, it can be seen from equations (6) that systematically varying the surface charge density will cause a change in the observed velocities. Systematic manipulation of surface charge density was carried out by changing the solution pH and surface functionalization. Results reported in the next few sections show the effects of each of the parameters on observed velocity trends in electrokinetic flows.

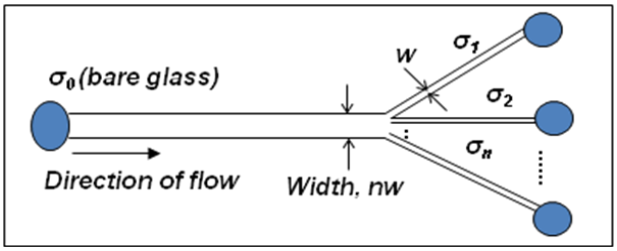

Figure 1: A schematic representation for the channel network used. Each exit channel is 50 μm wide and 1 cm long. The depth of the channel is 100 nm. Inlet channel is base glass and the exit channels are modified with different functionalization to alter the surface charge density, σ_i.

Experimental Methodology

Glass substrates (No. 2 cover glass, Corning) were patterned

with conventional UV lithography to generate the channel network shown in Figure 1. The channels were wet-etched using buffered oxide etch to yield channels with 100 nm depth. A Cr/Au layer was used as an etch mask for the glass etch step. As shown in Figure 1, each channel is 1 cm long and the exit channels are 50 μm wide. The inlet channel width is scaled to the number of exit channels to allow even flow rates in each channel under the case of no surface modification. Through holes were drilled in a top cover of the same type of glass and the two glass slides were then fusion bonded thermally at 110°C after a thorough clean. An SEM image of the channel cross-section is shown in Figure 2.

Figure 2: SEM image showing the cross-section of a bonded channel. Part of the slit-like channel with a channel depth of 100 nm is seen.

The channels were flushed with DI water and observed under a microscope to verify bonding and absence of leakage. After bonding, the surfaces were modified by a previously developed methodology [5]. Figure 3 shows the process for modifying the surfaces schematically. Briefly, first a self-assembled monolayer with a nucleophilic end-group (-Br) was deposited followed by a S_N2 nucelophilic substitution to generate an azido terminated surface followed by 'click' chemistry to create functionalized surfaces with pre-designed properties. The 'click' solutions of the aminated terminal alkyne (with propyl backbone) and the methylated alkyne (octyne) were prepared as 10 mM solutions in ethanol. Three surface terminations (-Br, -NH_2, and –CH_3) were tested in contrast to bare glass or unmodified surfaces. All experiments were conducted with a NaCl solution prepared in DI water at pH 7 ± 0.2 and obtained by titrating NaOH against HCl. The total electrolyte concentration for NaCl was 10 mM.

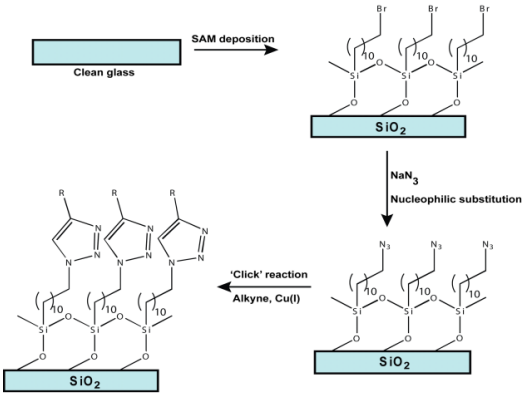

Figure 3: The schematic shows formation of surface layers through the 'click' process. The functionalizations discussed in this work include bare glass (-OH), brominated surfaces (-Br), aminated surfaces (-NH_2), and methylated surfaces (-CH_3)

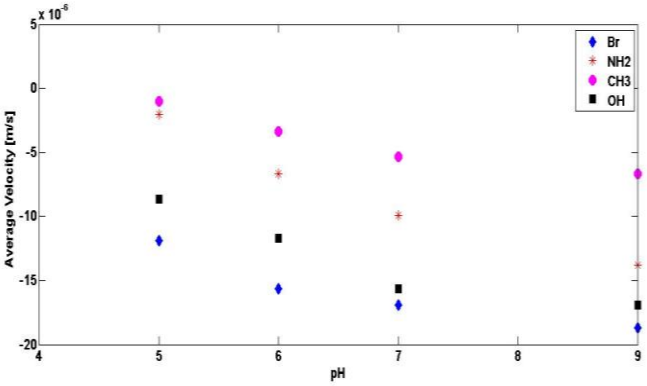

Figure 4: Average velocity as predicted by conventional 1-D electrokinetic model for slit-like channel. The velocity is plotted as function of pH, which regulates surface charge density.

RESULTS AND DISCUSSION

The model above describes electrokinetic flow in a slit-like channel. Figure 4 shows the average velocity in the nanochannel along the channel length (*z*-direction) as function of solution pH as predicted by the model.

Typically, in most cases surface charge density has also been reported to be increasing with pH. It can be seen from Figure 4 that the velocity increases in magnitude with increasing pH. Using the model, the pH dependence was further explored and $V_z(y)$ i.e. the axial velocity profile as function of channel depth is shown in Figures 5 and 6 for pH 3 and pH 9. It can be seen from Figure 5 that the velocity profile for the aminated and methylated surfaces are positive. This can be expected since at acidic pH the aminated surfaces are likely protonated and have a positive surface charge. The methylated surfaces have also been reported to acquire partial positive surface charge and thus the velocity profiles reflect the charge distribution. At 10 mM NaCl, the electric double layer is close to the walls and the 100 nm nanochannels behave like microchannels and the velocity profile is a plug-like flow, as shown by the plot. The velocity profiles for the bare-glass and brominated surfaces also show trends similar to those as expected.
One point to note from Figure 6 is the relative magnitude of the velocities. For example, comparing an aminated surface to the bare-glass surface it can be seen that at the center-point of the channel (location where velocity is maximum), the velocity for the aminated surface is lower in magnitude by approximately 22%; however, the surface charge density for an aminated surface

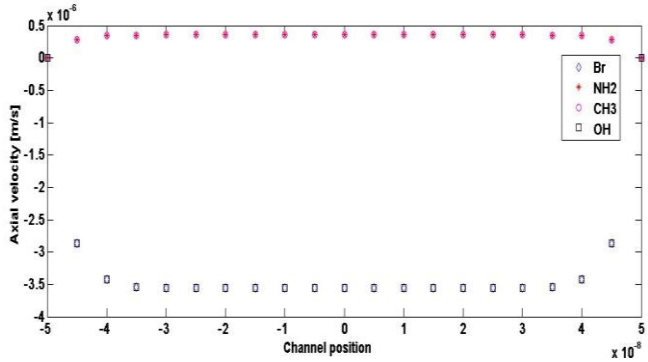

Figure 5: Velocity profile in a 100 nm channel at pH 3 for a 10 mM NaCl elelctrolyte as function of different surface functionalizations.

functionalized by the 'click' method is approximately 61% higher than that of a bare glass surface [8].

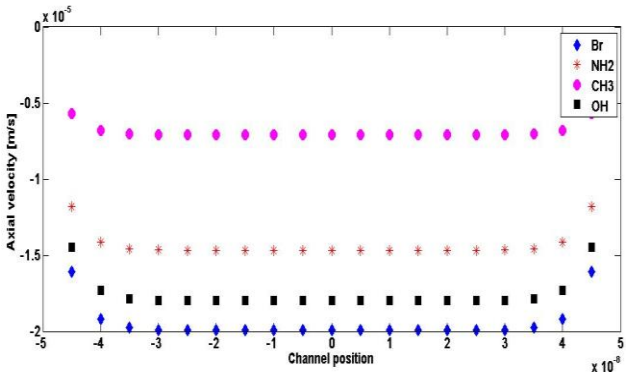

Figure 6: Velocity profiles in a 100 nm channel at pH 9 for a 10 mM NaCl electrolyte as function of different surface functionalizations.

The model described in the theoretical background permits an analysis that allows changing the channel critical dimensions and also the ionic concentration. Figure 7 shows the velocity profile for a channel with depth 20 nm at pH 9. It can also be seen from

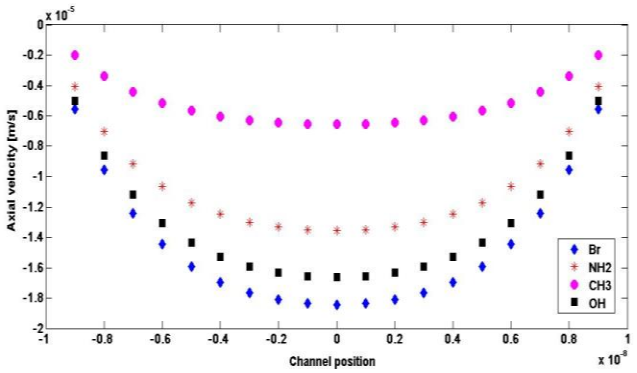

Figure 7: Velocity profiles in a 20 nm channel at pH 9 for a 10 mM NaCl electrolyte as function of different surface functionalizations.

Figure 7 that with the EDL occupying a larger fraction of the nanochannel the flow profile becomes more parabolic and the maximum velocity decreases in contrast to the values for the 100 nm channel.

Figure 8 presents another aspect of the theoretical analysis, which shows the effect at pH 9 by changing the concentration of the NaCl electrolyte. Since the EDL thickness scales inversely with the square root of concentration, Figure 8 shows the plot for the case of a 100 nm channel with a concentration of 0.4 mM. Figure 8 shows that by reducing the concentration by 25 times i.e. increasing the EDL by approximately 5 times in contrast to the case presented in Figure 6, the velocity profile becomes markedly more parabolic. In addition, the absolute magnitude of velocity is also observed to increase.

One of the main goals of the theoretical analysis was to determine conditions that can enable choice of conditions that will allow flow directing in the devices. Initial experiments with a 2-channel exit configuration show that with a surface charge difference of approximately 2.6 times between the exit channels (*cf.* Figure 1, $\sigma_2 = 2.6\sigma_1$). Figure 9 shows fluorescence data for two dyes, one positively charged (Rhodamine B) and one negatively charged (Fluorescein). It should be noted here that the fluorescein data is for a microchannel with depth at 10 μm as the negatively charged walls during experiments exclude the fluorescein, even for the 100 nm case with 10 mM NaCl i.e. conceptually similar to a microchannel. This suggests that the theoretical models are unable to predict the charge exclusion, even though they predict the correct plug-like flow profile for the small EDL case. Furthermore, the use of aqueous solutions also prevented any experiments with the hydrophobic methylated surfaces. Further experiments to contrast the influence of other polar solvents (e.g., alcohols) are currently underway to examine the role of surface modified devices for applications in flow control at the nanoscale.

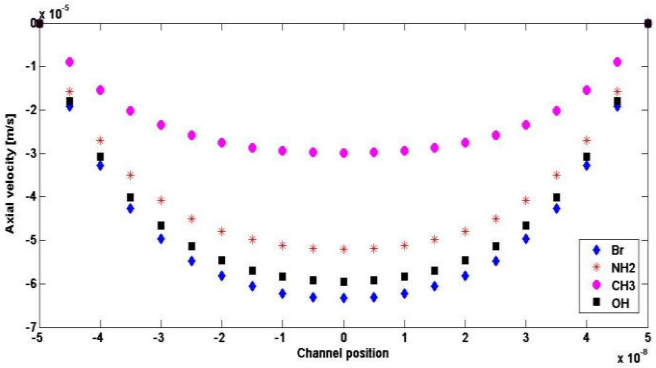

Figure 8: Velocity profiles in a 100 nm channel at pH 9 for 0.4 mM NaCl electrolyte as function of different surface functionalizations.

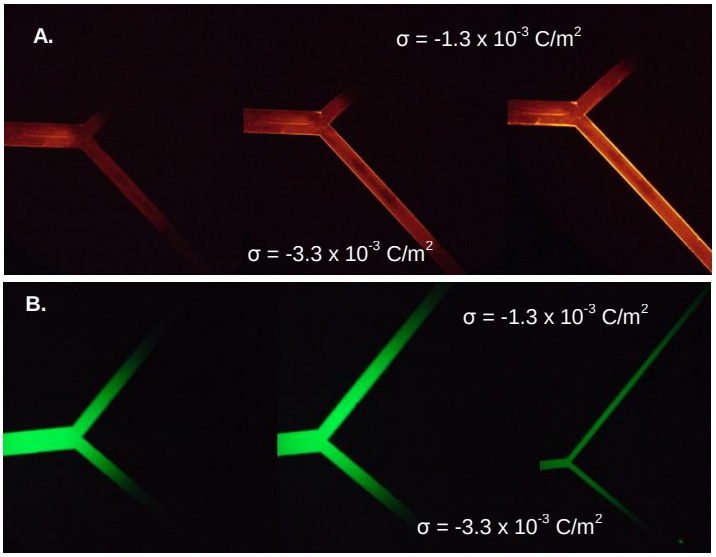

*Figure 9: **A**. $-NH_2$ (amine) functionalized microchannel shows a higher affinity for the positively charged dye (Rhodmaine B) at pH 7. Glass surfaces by contrast show less dye transport in time elapsed images. **B**. Same configuration as A but by contrast the channels with lower negative surface charge density in absolute magnitude show more affinity for Fluorescein (negatively charged dye). Total time elapse is approximately 400 s in images going from left to right.*

CONCLUSIONS

Results reported show that by systematically manipulating surface charge density surface mediated flow control can be achieved in nanochannels. Velocities in the channels change non-linearly with changes in surface charge as a consequence of chemical

modification. Even without interacting or overlapping EDLs, co-ions were excluded from the nanochannels as evidenced by fluorescein being excluded from the negatively charged channels while Rhodamine B did not show exclusion at the neutral pH during experiments. Theoretical models predict velocity profiles in agreement with previous reports; however, they fail to predict several subtleties as observed experimentally, including co-ion exclusion. The selective flow control demonstrated in this paper by use of chemically modified surfaces presents one avenue for development of 'valve-less' electrokinetic nanofluidic flow manipulation strategies.

REFERENCES

[1] M. Napoli, J.C.T. Eijkel, S. Pennathur, "Nanofluidic Technology for Biomolecule Applications: a Critical Review", Lab on a Chip, 10, 957, (2010).

[2] M. Gong, B.Y. Kim, B.R. Flachsbart, M.A. Shannon, P.W. Bohn, J.V. Sweedler, "An On-Chip Fluorogenic Enzyme Assay using a Multilayer Microchip Interconnected with Nanocapillary Array Membranes", IEEE Sensors Journal, 8, 601 (2008).

[3] J. Han, H.G. Craighead, "Separation of Long DNA Molecules in a Microfabricated Entropic Trap Array", Science, 288, 1026 (2000).

[4] S. Prakash, M.B. Karacor, S. Banerjee, "Surface Modification in Microsystems and Nanosystems", Surface Science Reports, 64, 233 (2009).

[5] S. Prakash, T.M. Long, J.C. Selby, J.S. Moore, M.A. Shannon, "'Click' Modification of Silica Surfaces and Glass Microfluidic Channels", Analytical Chemistry, 79, 1661 (2007).

[6] R. Karnik, R. Fan, M. Yue, D. Li, P. Yang, A. Majumdar, "Electrostatic Control of Ions and Molecules in Nanofluidic Transistors," Nano Letters, 5, 1633 (2005).

[7] D. Li,*Electrokinetics in Microfluidics*, Elsevier, Inc., Amsterdam, 2004.

[8] Y. Wu, M.B. Karacor, S. Prakash, M.A. Shannon, "Solid/Water Interface of Functionalized Silica Surface Studied by Dynamic Force Measurement", Proceedings of ASME 2010 3rd Joint US-European Fluids Engineering Summer Meeting and 8th International Conference on Nanochannels, Microchannels, and Minichannels, 2010, Paper number: FEDSM-ICNMM2010-30851.

CONTACT

*Shaurya Prakash, tel: +1-614-688-4045; prakash.31@osu.edu